BBA - Molecular Basis of Disease 1866 (2020) 165800

Contents lists available at ScienceDirect

BBA - Molecular Basis of Disease

journal homepage: www.elsevier.com/locate/bbadis

Myofibers deficient in connexins 43 and 45 expression protect mice from skeletal muscle and systemic dysfunction promoted by a dysferlin mutation

Gabriela Fernández[a], Guisselle Arias-Bravo[a,g], Jorge A. Bevilacqua[b,c], Mario Castillo-Ruiz[d,e], Pablo Caviedes[f,g], Juan C. Sáez[h,i,*], Luis A. Cea[a,**]

[a] Instituto de Ciencias Biomédicas, Facultad de Ciencias de la Salud, Universidad Autónoma de Chile, Santiago, Chile
[b] Departamento de Neurología y Neurocirugía, Hospital Clínico Univeridad de Chile y Departamento de Anatomía y Medicina legal, Facultad de Medicina, Universidad de Chile, Santiago, Chile
[c] Departamento de Neurología y Neurocirugía, Clínica Davila, y Corporacion de Investigaciones Neurológicas de Santiago (CINSAN), Santiago, Chile
[d] Escuela de Química y Farmacia, Facultad de Medicina, Universidad Andres Bello, Santiago, Chile
[e] Departamento de Ciencias Químicas y Biológicas, Facultad de Salud, Universidad Bernardo O Higgins, Santiago, Chile
[f] Programa de Farmacología, Instituto de Ciencias Biomédicas, Facultad de Medicina, Universidad de Chile, Santiago, Chile
[g] Centro de Biotecnología y Bioingeniería (CeBiB), Depto de Ingeniería Química, Biotecnología y Materiales, Fac. de Ciencias Físicas y Matemáticas, Universidad de Chile, Santiago, Chile
[h] Departamento de Fisiología, Fac. de Ciencias Biológicas, Pontificia Universidad Católica de Chile, Santiago, Chile
[i] Instituto de Neurociencias, Centro Interdisciplinario de Neurociencias, Universidad de Valparaíso, Valparaíso, Chile
[g] Instituto de Ciencias de la Salud, Universidad de O'Higgins, Rancagua, Chile

ARTICLE INFO

Keywords:
Calcium ion
Muscular dystrophy
Membrane permeability
Fat infiltration
Muscular performance

ABSTRACT

Dysferlinopathy is a genetic human disease caused by mutations in the gene that encodes the dysferlin protein (*DYSF*). Dysferlin is believed to play a relevant role in cell membrane repair. However, in dysferlin-deficient (blAJ) mice (a model of dysferlinopathies) the recovery of the membrane resealing function by means of the expression of a mini-dysferlin does not arrest progressive muscular damage, suggesting the participation of other unknown pathogenic mechanisms. Here, we show that proteins called connexins 39, 43 and 45 (Cx39, Cx43 and Cx45, respectively) are expressed by blAJ myofibers and form functional hemichannels (Cx HCs) in the sarcolemma. At rest, Cx HCs increased the sarcolemma permeability to small molecules and the intracellular Ca^{2+} signal. In addition, skeletal muscles of blAJ mice showed lipid accumulation and lack of dysferlin immunoreactivity. As sign of extensive damage and atrophy, muscles of blAJ mice presented elevated numbers of myofibers with internal nuclei, increased number of myofibers with reduced cross-sectional area and elevated creatine kinase activity in serum. In agreement with the extense muscle damage, mice also showed significantly low motor performance. We generated blAJ mice with myofibers deficient in Cx43 and Cx45 expression and found that all above muscle and systemic alterations were absent, indicating that these two Cxs play a critical role in a novel pathogenic mechanism of dysfernolophaties, which is discussed herein. Therefore, Cx HCs could constitute an attractive target for pharmacologic treatment of dyferlinopathies.

1. Introduction

Dysferlin is a 230 kDa membrane protein mostly expressed in adult skeletal muscle, but weakly expressed in myoblasts (myogenic precursor cells, [1]). In adult fiber, dysferlin is mainly localized in the sarcolemma [2,3], and forms part of the transversal tubule (T-tubule) membrane system [4]. However, it has also been localized in intracellular vesicles [2]. In addition, dysferlin expression has also been found in non-mechanically active tissues including endothelial cells, where its absence causes deficient trafficking of membrane-bound proteins, suggesting that dysferlin might mediate the trafficking of other proteins [5].

Dysferlin gene (*DYSF*) mutations lead to a group of muscular dystrophies known as dysferlinopathies (Limb-girdle muscular dystrophy 2B and Miyoshi myopathy) [6]. Clinically, dysferlinopathies manifest between the second and third decade of life in previously asymptomatic patients. At onset, most patients describe weakness in the lower extremities, difficulty in running or climbing stairs, sometimes

* Correspondence to: J.C. Sáez, Centro Interdisciplinario de Neurociencias, Universidad de Valparaíso, Pasaje Harrington 287, Playa Ancha, Valparaíso, Chile.
** Correspondence to: L.A. Cea, Av. Llano Subercaseaux 2801, San Miguel, Santiago, PO BOX 8910060, Chile.
E-mail addresses: juancarlos.saez@uv.cl (J.C. Sáez), luis.cea@uautonoma.cl (L.A. Cea).

https://doi.org/10.1016/j.bbadis.2020.165800
Received 4 October 2019; Received in revised form 18 March 2020; Accepted 10 April 2020
Available online 16 April 2020

accompanied with pain. These symptoms are usually accompanied by an increase of blood creatine kinase levels [7], suggesting increased myofiber destruction. Dysferlin is thought to participate in membrane repair after damage, which is a mechanism underlying the pathology that has been widely accepted [8,9].

Mutations in *DYSF* lead to the absence or reduction of dysferlin protein in skeletal muscles [2]. In attempts to further understand the role of dysferlin in pathological conditions, Lostal et al. [10] successfully recovered the membrane repairing function, which was accomplished by means of two strategies: 1) by generating transgenic mice that overexpressed myoferlin - a structural and functional homologous protein of dysferlin - that were later mated with dysferlin-null mice. The resulting animals recovered membrane repair capabilities, yet muscular degeneration progressed invariably; 2) by performing an AAV-mediated transfer of a minidysferlin, which is a domain of dysferlin previously shown to correct membrane repair deficits *in vitro*. This approach also failed to improve muscle histology and to arrest muscle wasting. Thus, the aforementioned evidences strongly suggest the existence of other pathological mechanisms triggered by the absence of dysferlin, in addition to deficient membrane repair.

In this regard, prior reports have determined the presence of inflammation signals in dysferlin-deficient skeletal muscles [11], dysregulation of intracellular free Ca^{2+} concentration in myofibers [8,12], increased oxidative stress in muscular tissue [13], the presence of adipose tissue in muscles [14,15], and alterations in T-tubule structure [9]. These changes have been shown to be ameliorated by reducing external [Ca^{2+}] or the blockade of L-type Ca^{2+} channels (DHPR) with diltiazem [4]. Since DHPR channels expressed in skeletal myofibers are voltage transducers poorly permeable to Ca^{2+} [16], it is likely that myofibers deficient in dysferlin express a different type of Ca^{2+} permeable channel inhibited by diltiazem. Moreover, the removal of external Ca^{2+} stabilizes T-tubule structure in myofibers deficient in dysferlin, suggesting the presence of an anomalous influx of extracellular Ca^{2+} mediated by membrane channels. In this context, previous reports have documented the expression of functional connexin hemichannels (Cx HCs) in mature human myotubes bearing *DYSF* mutations [17], which were deemed to be responsible for elevations of basal intracelular free Ca^{2+} concentration in these cells.

Cx HCs are hexameric channels formed by one or more types of connexins (Cxs). Some Cx HCs are known to be permeable to Ca^{2+} [18], which has also been associated to increased oxidative stress [19]. Cxs 39, 43 and 45 are expressed during the ontogeny and regeneration of muscles [20,21]. However, these proteins are undetectable in normal adult muscles [22–24], given that their expression is repressed by micro RNAs after myoblast fusion during myogenesis [25]. On the other hand, *de novo* expression of Cx HCs is known to mediate muscular atrophy in denervated muscles along with the activation of the inflammasome. This increases the production of proinflammatory cytokines (*e.g.*, TNF-α and IL-1β), and the activation of NFκB transcription factor, hence generating an inflammatory state in muscular tissue [23]. These responses have been shown to be accompanied by increased oxidative stress promoted by Cx HCs [26], and do not occur in myofibers deficient in Cx43 and Cx45 expression [23,27]. The expression of Cxs has also been shown to play a relevant role in muscle alterations induced by dystrophin mutation in mdx mice, a model of Duchenne muscular dystrophy [28]. Whether the above mechanisms apply to other conditions that induce muscular dystrophies, such as dysferlinopathies, remains to be studied.

In this report, we used blAJ animals (a dysferlinopathy model) cross-bred with mice deficient in Cx43 and Cx45 expression only in differentiated myofibers. In these animals, we studied the possible participation of Cx HCs in the development of muscular dystrophy. We found that the absence of Cxs prevents muscular deterioration and dysfunction exhibited by skeletal muscles in blAJ mice.

2. Materials and methods

2.1. Reagents

N-benzyl-p-toluene sulphonamide (BTS), FURA-2 AM, carbenoxolone and collagenase type I, suramine sodium salt and Evans blue (EB^{4-}) were obtained from Merck/Sigma-Aldrich (St. Louis, USA). Ethidium (Etd^{+}) bromide, DMEM/F12 medium and fetal bovine serum (FBS) were purchased from GIBCO/BRL (Grand Island, NY, USA). Fluoromount-G and 4 ‘,6-diamidino-2-fenilindol (DAPI) were obtained from Electron Microscopy Science (Hatfield, PA, USA). Monoclonal anti-Cx43 antibody (1:250) was purchased from BD Biosciences (San Jose, CA, USA) and polyclonal anti-Cx45 antibody (1:250) was purchased from Invitrogen (Carlsbad, CA, USA). Polyclonal anti-Cx39 antibody (1:500) was obtained from Invitrogen, and anti-mouse IgG antibodies-conjugated to Cy3 (1:300) were purchased from Jackson Immunoresearch laboratories (West Grove, PA, USA). Monoclonal anti-dysferlin antibody (1:250) was obtained from Cell Signaling (Danvers, MA, USA).

2.2. Animals

Male 7–8 months-old mice were used for this study. C57 Bl6 wild type (wt) and $Cx43^{fl/fl}$ $Cx45^{fl/fl}$ mice were used as control mice and $Cx43^{fl/fl}$ $Cx45^{fl/fl}$:Myo-Cre (M-C) mice, which do not express Cxs 43 and 45 in skeletal myofibers after myogenin expression, were generated by mating $Cx43^{fl/fl}$ and $Cx45^{fl/fl}$ mice with Myo-Cre mice, which express Cre recombinase under the control of the myogenin promoter (MYF4) and the MEF2C enhancer [29]. In addition, we used blAJ mice, which bear a homozygous mutation in the *DYSF* gene (encoding dysferlin) in which the dysferlin protein is undetected (Kindly donated by Jain Foundation, USA). We also generated blAJ $Cx43^{fl/fl}Cx45^{fl/fl}$ as control mice of genetic manipulation applied to the genetation of blAJ $Cx43^{fl/fl}$ $Cx45^{fl/fl}$:M-C mice, which do not express dysferlin, Cx43 and Cx45 in skeletal myofibers. These animals were obtained by crossing a male $Cx43^{fl/fl}$ $Cx45^{fl/fl}$ with a female blAJ mice and by crossing a male $Cx43^{fl/fl}$ $Cx45^{fl/fl}$:M-C with a female blAJ mice, respectively.

2.3. Western blot analysis

The relative amounts of Cx proteins were determined as previously described [28]. In brief, tendon-free gastrocnemius muscles were minced in small pieces and then homogenized (homogenizer; Brinkmann) and sonicated (Heat Systems Microson). Tissue homogenates were centrifuged for 15 min at 13,000 × *g* and pellets were discarded. Supernadant samples were processed for Western blot analyses of proteins of interest. Blots were incubated overnight with appropriate dilutions of primary antibodies diluted in 5% fat free milk–PBS solution. Then, blots were rinsed with 1% PBS solution–Tween 20 and incubated for 40 min at room temperature with HRP-conjugated goat anti-rabbit or anti-mouse IgGs (Santa Cruz Biotechnology). After several rinses, immunoreactive proteins were detected using ECL reagents according to the manufacturer's instructions (PerkinElmer).

2.4. Isolation of mouse skeletal myofibers

Myofibers were extracted as previously described by [23]. Briefly, undamaged myofibers were dissociated from *flexor digitorum brevis* (FDB) muscles (fast muscles). The plantaris tendons and connective tissue were removed from anesthetized mice. Then, FDB muscles were carefully dissected and immersed in culture medium (DMEM/F12 supplemented with 10% FBS) containing 0.2% type I collagenase, incubated for 3 h at 37 °C, and transferred to a 15-mL test tube (Falcon) containing 5 mL of culture medium, in which muscle tissue was gently triturated 10 times by using a Pasteur pipette with a wide tip to disperse single myofibers. Dissociated myofibers were centrifuged at 1,000 rpm

for 15 s (centrifuge model 8700; Kubota) and washed twice by sedimentation: first with PBS 1 × solution and then with Krebs buffer (in mM: 145 NaCl, 5 KCl, 3 $CaCl_2$, 1 $MgCl_2$, 5.6 glucose, 10 Hepes-Na, pH 7.4) containing 10 μM BTS (a contraction inhibitor) to reduce muscle damage during the isolation procedure. Finally, fibers were resuspended in 5 mL of Krebs Hepes buffer containing 10 μM BTS, plated in plastic culture dishes or placed in 1.5-mL Eppendorf tubes, and kept at room temperature.

2.5. Evans blue uptake in vivo assay

This procedure was performed as described previously [23]. In brief, animals were injected i.p. 6 h before euthanasia with Evans blue (EB^{4-}, 80 mg/kg) dissolved in a sterile saline solution. To inhibit the *in vivo* EB^{4-} uptake by myofibers, Cbx (80 mg/kg), a nonselective Cx hemichannel blocker, was administered (i.p.) 20 min before the EB^{4-} injection. Then, animals were euthanized. *Gastrocnemius* muscles were dissected and fast-frozen in isopentane precooled in liquid nitrogen, and EB^{4-} fluorescence intensity was quantified in muscle cross-sections in intracellular regions by image processing performed offline with ImageJ software (National Institutes of Health) and the images were obtained by using a conventional Nikon Eclipse Ti fluorescent microscope (λ excitation, 545 nm; λ emission, 595 nm).

2.6. Time-lapse recording of Etd^+ uptake

Cellular uptake of Etd^+ was evaluated by time-lapse measurements as previously described [24]. Briefly, freshly isolated myofibers plated onto plastic culture dishes were washed twice with Krebs buffer solution. For timelapse measurements, myofibers were incubated in recording medium containing 5 μM Etd^+. Etd^+ fluorescence intensity was recorded in regions of interest that corresponded to myofiber nuclei by using a water immersion Olympus 51W1I upright microscope (Japan). Images were captured with a Retiga 13001 fast-cooled monochromatic digital camera (12-bit; QImaging) every 30 s, and image processing was performed offline with ImageJ software (National Institutes of Health).

2.7. Intracellular Ca^{2+} signal

Basal intracellular Ca^{2+} signal was evaluated in isolated myofibers using FURA 2-AM ratiometric dye. Myofibers were incubated in Krebs-Ringer solution (in mM: 145 NaCl, 5 KCl, 3 $CaCl_2$, 1 $MgCl_2$, 5.6 glucose, 10 HEPES-Na, pH 7.4) containing FURA2-AM dye (2 μM) for 45 min at room temperature. Then, the Ca^{2+} signal was measured in a Nikon Eclipse Ti microscope equipped with epifluorescence illumination, and images were obtained by using a Clara camera (Andor) at 2 wavelengths of (λ) 340 nm and 380 nm, calculating the ratio of fluorescence emission intensity after stimulation with each one of these two wavelengths.

2.8. Immunofluorescence analysis

We used a protocol described previously [23]. Briefly, muscles were fast frozen with isomethylbutane cooled in liquid nitrogen. Then, cross-sections (10 μm) were obtained by using a cryostat and fixed with 4% formaldehyde for 10 min at room temperature. Sections were incubated for 3 h at room temperature in blocking solution (50 mM NH_4Cl, 0.025% Triton, 1% BSA on PBS solution 1 ×), incubated overnight with appropriate dilutions of primary antibody, washed five times with PBS 1 × solution followed by 1 h incubation with secondary antibody conjugated to Cy2 or Cy3, and mounted in Fluoromount G. Immunoreactive binding sites were localized under a Nikon Eclipse Ti microscope equipped with epifluorescence illumination, and images were obtained by using a Clara camera (Andor).

2.9. Cross sectional area (CSA) measurements

The CSA of skeletal muscle fibers was evaluated in cross sections of muscles fixed with 4% (wt/vol) paraformaldehyde and stained with hematoxylin-eosyn, as described previously [23]. The CSA of myofibers was evaluated by using offline analyses by ImageJ software (National Institutes of Health).

2.10. Creatine kinase (CK) activity measurement

Blood was obtained from old mice (32–36 weeks of age). The collected blood was incubated (45–60 min) at 37 °C to allow blood to clot. Then, samples were centrifuged (1,000 rpm for 5 m) to remove the clot, and the clear supernatant corresponding to the serum was obtained. The catalytic activity of serum creatine kinase was determined at 37 °C on a spectrophotometer at 340 nm in accordance with the manufacturer's instructions (Valtek S.A., Santiago, Chile).

2.11. Hematoxylin-eosyn stain

This staining was carried out as previously described [27]. Briefly, fixed cross sections of GC muscles, mounted on glass slides were stained with hematoxylin during 5 min and rinsed with hematoxylin rinsing vat. Then, samples were stained with eosin for 10 min and rinsed with water.

2.12. Oil red staining O

This staining was carried out as previously described [30]. Briefly, cross sections of GC muscles mounted on glass slides were fixed with 4% paraformaldehyde in the presence of 180 mM $CaCl_2$. After that, oil red O reagent was added and after 30 min the exccess was removed, and the samples were rinsed with water.

2.13. Physical exercise test (rotarod)

A group of mice was subjected to running in the drum of the rotarod apparatus placed at a height of 40 cm. A sponge bedding was placed underneath the apparatus to receive the animals upon falling from the apparatus. Performance consisted of the following: after an adaptation period of 5 min, the apparatus increased its velocity, starting at 5 rotations per minutes (RPM) and increasing by 5 RPMs every 20 s until the animals fell. This protocol was tried 3 times with a rest period of 2 min between trials for each animal and evaluated once a week during nine weeks.

3. Results

3.1. Connexin proteins are expressed by mouse dysferlin-deficient myofibers

As previously stated, Cx40.1, Cx43 and Cx45 have been detected in muscular biopsies from adult human patients bearing mutations in *DYSF*, but not in biopsies from patients without a muscular pathology [17,28]. Hence, we evaluated whether these Cxs are present in samples of adult gastrocnemius muscles from dysferlin-deficient mice (blAJ type mice, an animal model of dysferlinopathy). While gastrocnemius muscles from wild type mice did not present immunoreactivity to Cx39, Cx43 and Cx45 (Fig. 1), of blAJ and blAJ $Cx43^{fl/fl}Cx45^{fl/fl}$ mice showed strong Cx39 (orthologous of human Cx40.1), Cx43 and Cx45, immunoreactivity, which exhibited greater fluorescence intensity in the contour of myofibers (green signal) (Fig. 1A), suggesting their presence in the sarcolemma. This is also in line with the possible presence of Cx HCs in these skeletal muscle fibers. In addition, we evaluated the presence of Cx proteins in cryosections of gastrocnemius muscle from blAJ mice deficient in Cx43 and Cx45 in myofibers after myogenin expression (blAJ $Cx43^{fl/fl}Cx45^{fl/fl}$:M-C mice). In these muscles, only the Cx39

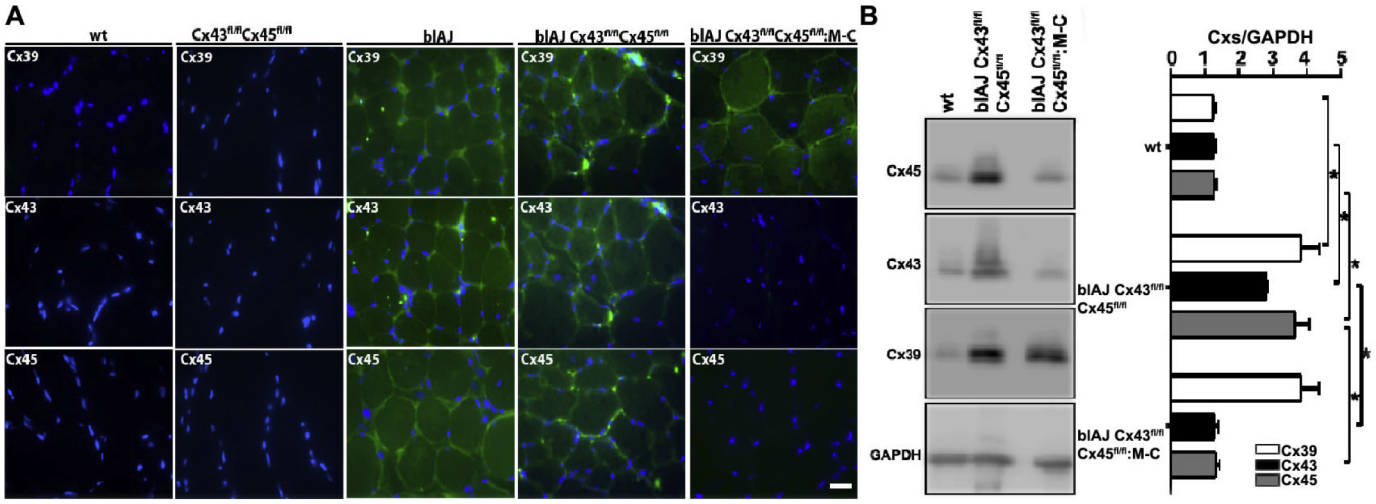

Fig. 1. Dysferlin deficient skeletal myofibers express connexin proteins. *Gastrocnemius* (GC) muscles from 8-month-old animals that express dysferlin (wild type: wt and Cx43$^{fl/fl}$Cx45$^{fl/fl}$ mice), mice deficient in dysferlin expression (blAJ and blAJ Cx43$^{fl/fl}$Cx45$^{fl/fl}$ mice) and mice deficient in dysferlin expression as well Cx43 and Cx45 expression (blAJ Cx43$^{fl/fl}$Cx45$^{fl/fl}$:M-C mice). Muscles were dissected and cyopreserved. A, Cryosections of this muscle were used to evaluate the presence and distribution of connexin proteins by immunofluorescence analysis. Pannels show Cx39, Cx43 and Cx45 immunoreactivity (green signal) and nuclei stained with DAPI (blue signal). B, Western blot analysis of Cx39, Cx43 and Cx45 protein abundance in GC muscles. Scale bar: 50 μm (representative fields obtained in 5 section of each animal; $n = 6$ mice).

protein was detected, which indicates that the inducible knockout of Cx43 and Cx45 in these mice was successful. In addition, we determined the relative amount of Cx39, Cx43 and Cx45 proteins by Western blot analysis in gastrocnemius (GC) muscles from wt, blAJ Cx43$^{fl/fl}$Cx45$^{fl/fl}$ and blAJ Cx43$^{fl/fl}$Cx45$^{fl/fl}$:M-C mice, observing that in blAJ muscles the relative amount of Cx39 (3.83 ± 0.51), Cx43 (2.83 ± 0.01) and Cx45 (3.68 ± 0.32) were significantly higher as compared to wt muscles. These changes were not elicited in muscles of blAJ Cx43$^{fl/fl}$Cx45$^{fl/fl}$:M-C for Cx43 (1.25 ± 0.03) and Cx45 (1.29 ± 0.04) but Cx39 (3.82 ± 0.45) persisted higher than wt muscles (Fig. 1B). Also, a weak signal for Cx39 (1.21 ± 0.01), Cx43 (1.22 ± 0.01) and Cx45 (1.24 ± 0.01) proteins was detected in wt muscles. Keeping in mind that blAJ Cx43$^{fl/fl}$Cx45$^{fl/fl}$:M-C mouse is a constitutive Cx43 and Cx45 KO only in skeletal myofibers, the weak signal detected in whole muscle samples could be explained by the expression of these two Cxs by other cell types found in muscular tissue, like vascular cells [31,32].

Since muscles and motor function of blAJ and blAJ Cx43$^{fl/fl}$Cx45$^{fl/fl}$ mice were equivalent only data obtained with blAJ Cx43$^{fl/fl}$Cx45$^{fl/fl}$ mice will be presented as model of dysfernilopathy in the rest of the manuscript.

3.2. Functional Cx HCs hemichannels are expressed in vivo and in vitro in skeletal muscle fibers

Since Cx proteins were detected in the skeletal muscles of dysferlin-deficient mice (Fig. 1), we then studied if myofibers expressed functional Cx HCs *in vivo* by using the Evans blue (EB^{-4}) uptake assay. To this end, 7 month old control and blAJ mice of different ages (3, 7 and 9 months old) were injected intraperitoneally (i.p.) with EB^{-4}, and after 6 h the mice were euthanized. *Gastrocnemius* muscles were dissected and processed for cryosections. Muscle cryosections were then analyzed by fluorescence microscopy. EB^{4-} staining was detected in the cell interior of few myofibers in sections of 3 month old blAJ mice (6.72 ± 1.41), which was clearly noticeable in all myofibers from 7 (28.11 ± 0.41) and 9 (27.93 ± 0.42) month old mice (Fig. 2). In contrast, control muscles of 7 month old mice showed EB^{-4} fluorescence only in the extracellular space that surrounded the myofibers (4.12 ± 1.05). This suggests that the dye reached the interstitial space, but did not cross the sarcolemma (Fig. 2, fluorescent field and graph). Similarly, muscle sections from mice pretreated with the non-selective hemichannel blocker carbenoxolone (9.11 ± 0.71) (blAJ + Cbx) or blAJ mice with myofibers deficient in Cx43 and Cx45 expression (5.29 ± 0.93) (blAJ Cx43$^{fl/fl}$Cx45$^{fl/fl}$:M-C) did not show EB^{4-} staining in myofiber cytoplasm (Fig. 2, fluorescent fields and graph). Also, and in order to corroborate that the EB^{-4} uptake was mediated by membrane channels such as Cx HCs and is not due a loss of sarcolemma integrity, we evaluated the uptake of rhodamine dextran, a high molecular weight dye (10,000 Da) excluded by Cx HCs [26], observing that there is no entry of this dye (red signal) in the myofibers from 8 month old blAJ mice (Suppl. Fig. 1). Therefore, the results can be explained by increase in sarcolemma permeability by Cx HCs and the sarcolemma is not torn up.

In addition, we evaluated whether the sarcolemma from freshly isolated myofibers presented altered permeability. This analysis was performed by using the ethidium (Etd^{+}) uptake assay [23,24] in freshly isolated myofibers from control and blAJ mice. We observed that myofibers from blAJ Cx43$^{fl/fl}$Cx45$^{fl/fl}$ mice exhibited significantly higher Etd^{+} uptake (1.26 ± 0.25) compared to that detected in wt myofibers (0.41 ± 0.05) and in blAJ myofibers deficient in Cx43 and Cx45 expression (0.51 ± 0.02) (Fig. 3A). Furthermore, the Etd^{+} uptake rate of blAJ Cx43$^{fl/fl}$Cx45$^{fl/fl}$ myofibers was blocked by carbenoxolone (Cbx, 0.47 ± 0.12) (Fig. 3B), indicating that Cx HCs were functional under basal conditions. In contrast, myofibers from (blAJ Cx43$^{fl/fl}$Cx45$^{fl/fl}$:M-C), showed Etd^{+} uptake rate comparable to those of control myofibers and was unaffected by Cbx (Fig. 3B).

3.3. Cx HCs play a critical role in elevated values of basal intracellular Ca^{2+} signal

Since dysferlin-deficient myofibers express functional Cx HCs, which are permeable to Ca^{2+} [18], it is likely that these myofibers present elevated basal intracellular Ca^{2+} signals similar to those seen in mdx mice, a model of Duchenne muscular dystrophy [28]. We evaluated intracellular Ca^{2+} signal in wt and blAJ myofibers using the FURA 2-AM probe and found that the blAJ Cx43$^{fl/fl}$Cx45$^{fl/fl}$ myofibers exhibit significantly higher basal Ca^{2+} signals (0.61 ± 0.01, ~20%) compared to wt (0.47 ± 0.025) or blAJ Cx43$^{fl/fl}$Cx45$^{fl/fl}$: M-C myofibers (0.46 ± 0.02) (Fig. 4), suggesting that the absence of Cx43 and Cx45 is sufficient to prevent the increase in Ca^{2+} signal observed in the

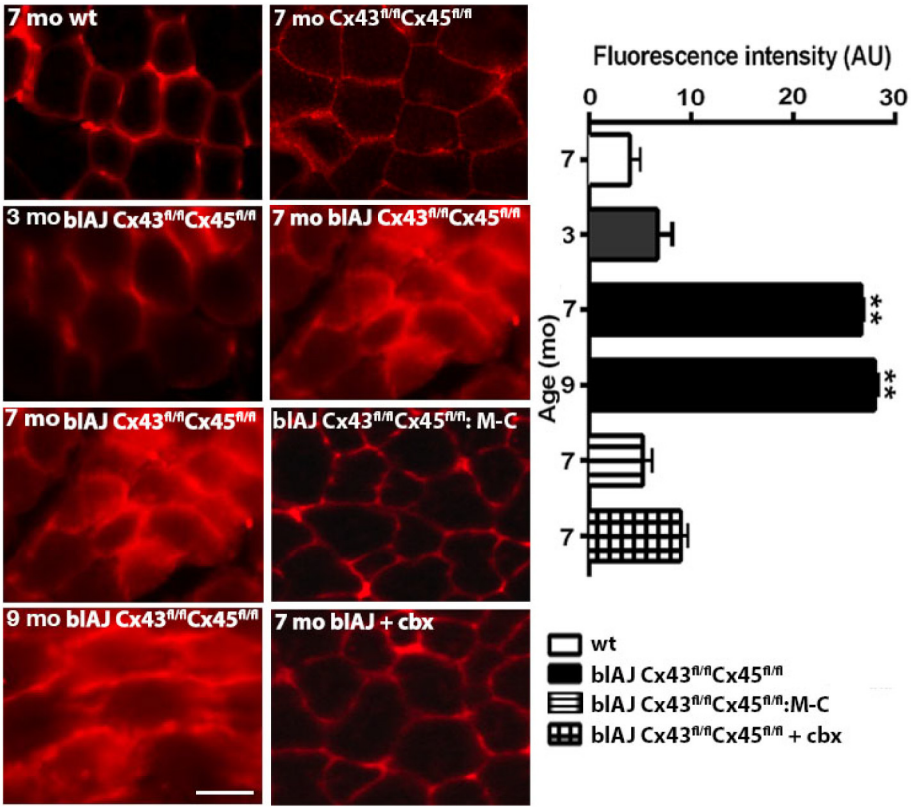

Fig. 2. The sarcolemma permeability of myofibers from muscles of dysferlin deficient mice is increased and is normalized upon inhibition of Cx HCs or lack of Cx43 and Cx45 expression. Wild type mice (7 months old), $Cx43^{fl/fl}Cx45^{fl/fl}$ (7 months old), blAJ $Cx43^{fl/fl}Cx45^{fl/fl}$ mice of different ages (3, 7 and 9 month old) or 7 month old animals acutely treated with carbenoxolone (blAJ $Cx43^{fl/fl}Cx45^{fl/fl}$ + cbx), and 7 month old dysferlin deficient mice with myofibers deficient in Cx43 and Cx45 expression (blAJ $Cx43^{fl/fl}Cx45^{fl/fl}$:M-C mice) were used. All animals were injected intraperitoneal with Evans blue (EB, 80 mg/kg) and after 6 h, they were euthanized, and the TA muscles were dissected. Then, cryosections (thickness 10 μm) were obtained, mounted in microscope slides, analyzed by fluorescence microcopy (excitation $\lambda = 530$ nm, emission $\lambda = 590$ nm) and the fluorescence intensity was recorded inside the myofibers (Graph). Dark fields show fluorescence images of muscle sections of each animal condition described above. The graph illustrates the EB uptake in each condition (bottom right panel). Values represent means ± SEM. Scale bar: 50 μm (n = 6 animals). $^{**}P < 0.01$ compared to all conditions. Between muscles from blAJ $Cx43^{fl/fl}$ $Cx45^{fl/fl}$ 7 and 9 month old there is no significant differences.

model of dysfernilopathy.

3.4. The absence of Cx HCs prevents skeletal muscle degeneration induced by dysferlin deficiency

Considering that basal intracellular Ca^{2+} signal was found to be elevated in blAJ $Cx43^{fl/fl}Cx45^{fl/fl}$ myofibers, and that this divalent cation activates several degradative pathways [33,34], we decided to analyze features of skeletal muscle deterioration. To accomplish this goal, we studied four parameters: 1) the number of non-peripheral nuclei as a measure of new myofibers generated to replace damaged ones [35]; 2) cross sectional area (CSA) of fully myofibers with peripheral nuclei as measure of atrophy [28]; 3) creatine kinase (CK) activity in serum as an indicator of sarcolemma integrity; and 4) the presence of lipid accumulation within muscles, which is universally regarded as muscle tissue replacement by adipose tissue [14]. We found that muscles of blAJ $Cx43^{fl/fl}Cx45^{fl/fl}$ mice presented a significantly higher number of myofibers with internal nuclei (~30% of non-peripheral nuclei) as well as myofibers with clear reduction in CSA (~50%) as compared to control cells (Fig. 5). These deleterious changes were absent in blAJ muscles with myofibers deficient in Cx43 and Cx45 expression (blAJ $Cx43^{fl/fl}Cx45^{fl/fl}$:M-C mice), which did not differ from control values (Fig. 5). In addition, CK activity was elevated in serum from blAJ $Cx43^{fl/fl}Cx45^{fl/fl}$ animals (0.68 ± 0.004), but not in myofibers of blAJ $Cx43^{fl/fl}Cx45^{fl/fl}$:M-C (0.17 ± 0.02) mice (Fig. 6). Moreover, oil red O staining revealed lipid vesicles of variable sizes in muscles of blAJ $Cx43^{fl/fl}Cx45^{fl/fl}$ mice, but not in muscles of blAJ $Cx43^{fl/fl}Cx45^{fl/fl}$:M-C mice or muscles of wt mice (Fig. 7).

3.5. Remotion of Cxs 43 and 45 recovers dysferlin immunoreactivity

Considering that the absence of Cx43 and Cx45 prevented the increase of basal intracellular free Ca^{2+} signals (Fig. 4) and reduced muscular atrophy (Fig. 5), it was possible to infer that protein degradation pathways were not activated and prevent degradation of dysferlin. Therefore, we analyzed whether dysferlin protein could be

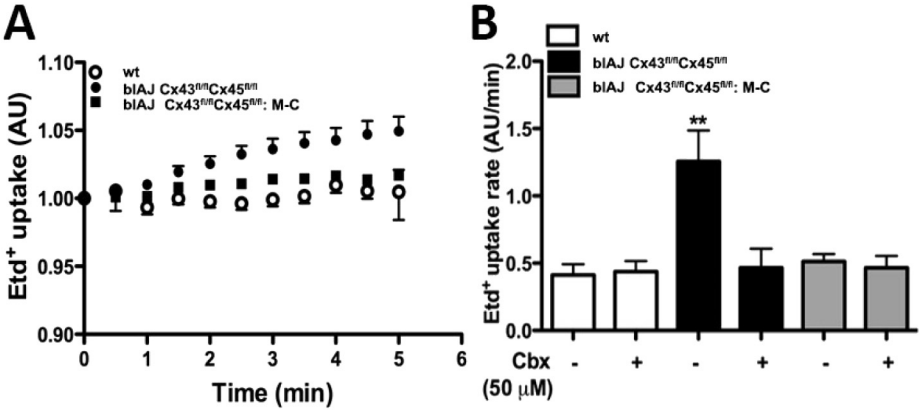

Fig. 3. Increased sarcolemma permeability of freshly isolated blAJ myofibers is prevented by the absence or inhibition of Cx HCs. Skeletal muscle fibers were isolated from flexor digitorum brevis muscle from wild type (wt, white bars), blAJ $Cx43^{fl/fl}Cx45^{fl/fl}$ (black bars) and blAJ $Cx43^{fl/fl}Cx45^{fl/fl}$:M-C mice (grey bar) mice. In these myofibers, ethidium (Etd^+) uptake was evaluated in absence or presence of carbenoxolone (Cbx), a non-selective Cx HC blocker, in time lapse experiments. A, representative curve of Etd^+ uptake over time in isolated myofibers. B, Etd^+ uptake rate obtained from slopes of curves similar to A. values represent means ± SEM. $^{**}P < 0.01$ respect to all conditions ($n = 4$ animals and 20 myofibers from each animal).

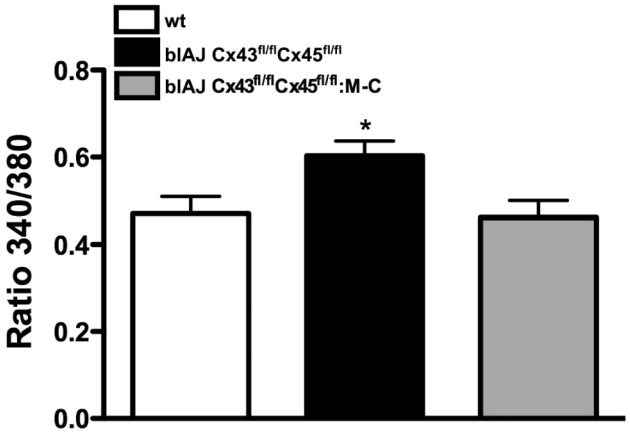

Fig. 4. Absence of Cx43 and Cx45 expression prevents the increase in basal intracellular Ca^{2+} signal of myofibers expressing mutated dysferlin. Skeletal myofibers were isolated from FDB muscle of wt (white bar), blAJ $Cx43^{fl/fl}Cx45^{fl/fl}$ (black bar) and blAJ $Cx43^{fl/fl}Cx45^{fl/fl}$:M-C (grey bar) mice. All mice used were 8 month old. Myofibers were incubated with FURA 2-AM probe and the Ca^{2+} signal evaluated as ratio of fluorescence emission at 340 and 380 nm. Then, the ratio between the signals obtained at 340 *versus* 380 nm was calculated. *$P < 0.05$ blAJ $C43^{fl/fl}Cx45^{fl/fl}$ statiscally significant *versus* wt and blAJ $Cx43^{fl/fl}$ $Cx45^{fl/fl}$ M-C ($n = 4$ animals and 20 myofibers for each animal). Each value corresponds to means ± SEM.

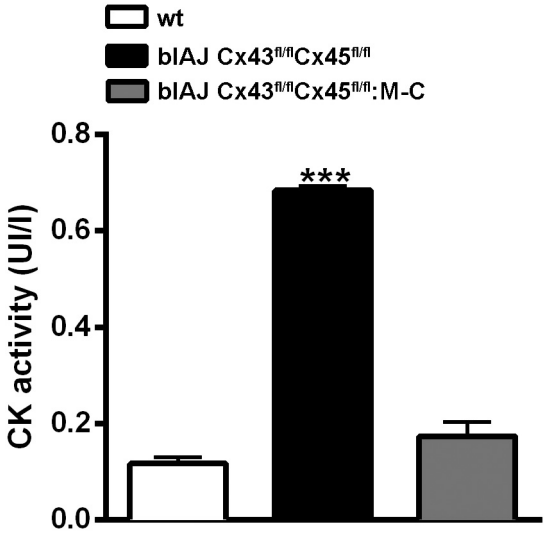

Fig. 6. Removal of connexin hemichannels prevents the elevation of serum creatine kinase activity in dysferlin deficient mice. The serum creatine kinase (CK) activity was evaluated in wild type (wt), blAJ $Cx43^{fl/fl}Cx45^{fl/fl}$ and blAJ $Cx43^{fl/fl}Cx45^{fl/fl}$:M-C mice. Note the significant elevation of serum CK activity in dysferlin deficient mice compared to control and blAJ $Cx43^{fl/fl}Cx45^{fl/fl}$:M-C mice. Values represent means ± SEM. $n = 4$; ***P < 0.01 respect to control mice.

detected in skeletal muscles in myofibers deficient in Cx43 and Cx45 expression. Dysferlin was clearly detected by immunofluorescence in myofibers of wt animals but was undetectable in myofibers of blAJ $Cx43^{fl/fl}Cx45^{fl/fl}$ mice (Fig. 8A). As predicted, in blAJ myofibers deficient in Cx43 and Cx45 expression a strong dysferlin reactivity similar to that detected in muscles of wt mice was found (Fig. 8A). Consistently, Western blot analysis revealed a clear band of ~230 kDa, compatible with the previously reported molecular weight to dysferlin

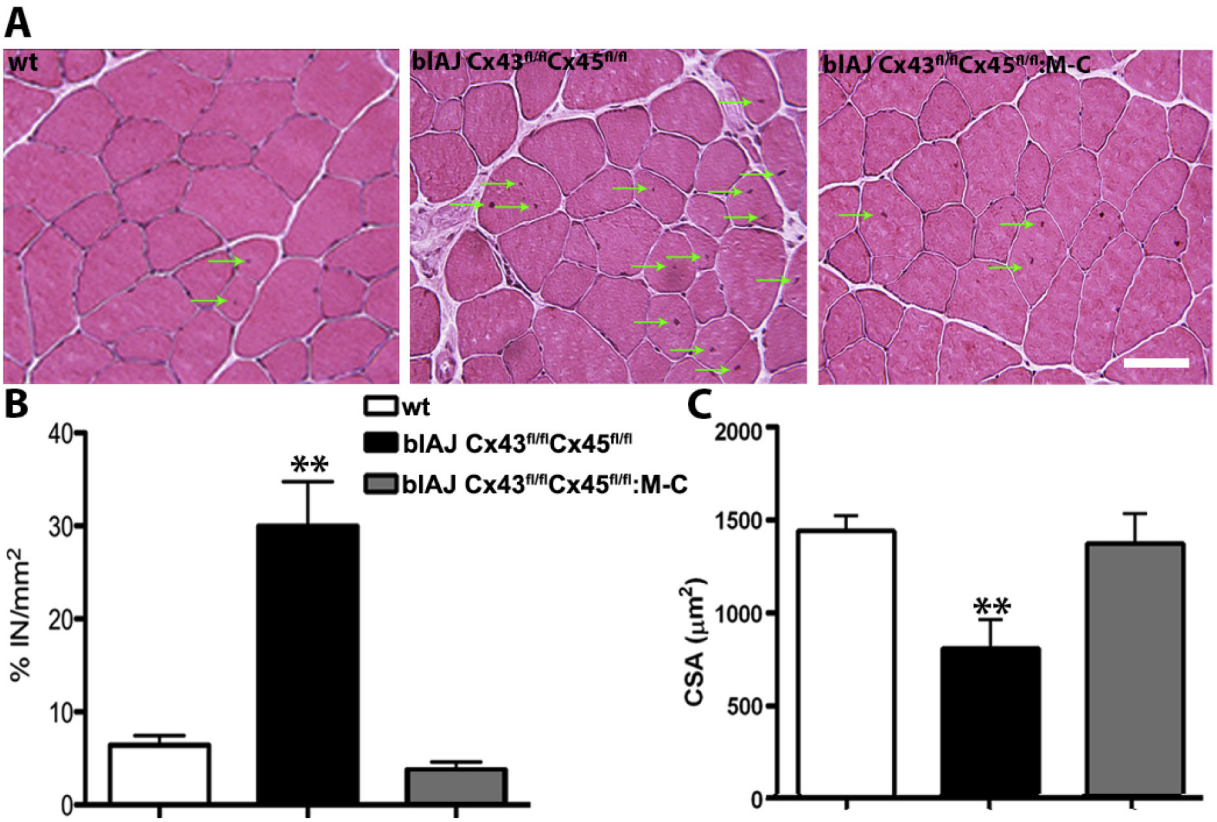

Fig. 5. Absence of connexin hemichannels prevents the increase of internal nuclei and CSA reduction in blAJ muscles. A. Hematoxylin-eosin staining was performed in gastrocnemius muscles sections from wild type (wt; white bar), blAJ $Cx43^{fl/fl}Cx45^{fl/fl}$ (black bar) and blAJ $Cx43^{fl/fl}Cx45^{fl/fl}$:M-C (grey bar) mice, and the presence of internal nuclei (green arrows) and cross-sectional area (CSA) of myofibers were quantified. B. Quantification of the number of internal nuclei. C. Quantification of CSA of myofibers as those shown in A. Values represent means ± SEM. **$P < 0.01$ respect to all conditions.

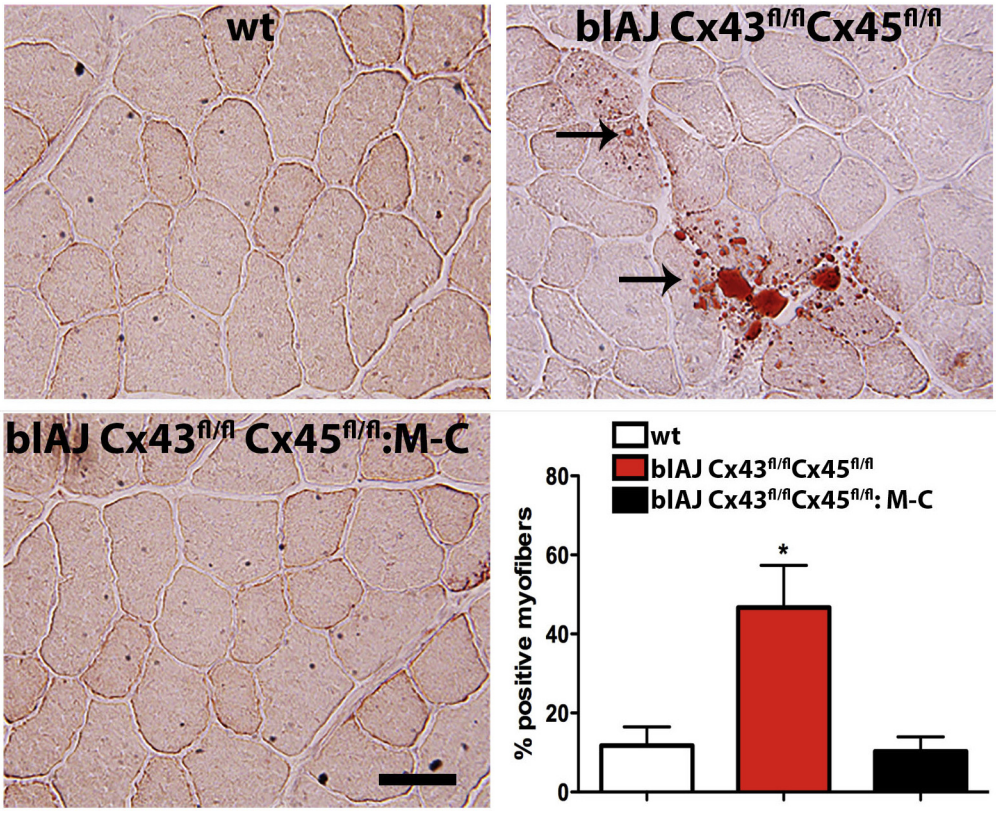

Fig. 7. Connexin hemichannels deficiency prevents lipid accumulation in muscles of dysferlin deficient mice. Cryosections of gastrocnemius muscles from wild type (wt), blAJ C43$^{fl/fl}$Cx45$^{fl/fl}$, and blAJ Cx43$^{fl/fl}$Cx45$^{fl/fl}$:M-C mice were analyzed for lipid accumulation using oil red O staining. Positive reactivity was only encountered muscles deficient only in dysferlin that express Cxs (top right panel: blAJ Cx43$^{fl/fl}$Cx45$^{fl/fl}$ mice) and was absent in muscle of wt (top left) and in muscles of mice deficient in Cx43, Cx45 and dysferlin (bottom left panel). Graph shows the quantification of the percentage of myofibers with oil red O positive signal from images showed in A, B and C. Values represent means ± SEM. $n = 4$; *$P < 0.05$ respect to all conditions.

[2], in total muscle homogenates from blAJ and blAJ Cx43$^{fl/fl}$Cx45$^{fl/fl}$:M-C, but this band was not detected in muscles of blAJ Cx43$^{fl/fl}$Cx45$^{fl/fl}$:M-C mice (Fig. 8B).

3.6. Reduced performance of blAJ animals in a functional test is a consequence of Cx43 and Cx45 HCs present in skeletal myofibers

After determining that muscles of the animal model of dysfernilopathy undergo damage due to the presence of Cx43 and Cx45 HCs, we analyzed if impaired performance in a functional rotarod test is a consequence of the HCs expression. We therefore evaluated the performance of wt, blAJ Cx43$^{fl/fl}$Cx45$^{fl/fl}$ and blAJ Cx43$^{fl/fl}$Cx45$^{fl/fl}$:M-C mice. We found that blAJ Cx43$^{fl/fl}$Cx45$^{fl/fl}$ mice performed worse (around 60% less) than wt mice, as was previously reported [36]. Interestingly, blAJ mice lacking Cx43 and Cx45 expression in myofibers showed a performance similar to that of wt mice in the rotarod test (Fig. 9), indicating that these channels play a critical role in the reduced motor performance of dysferlinopathy model. In addition, deficient expression of either Cx43 or Cx45 (blAJ Cx43$^{fl/fl}$:M-C and blAJ Cx45$^{fl/fl}$:M-C mice, respectively) only caused a partial improvement of the performance in rotarod test as compared to wt and blAJ Cx43$^{fl/fl}$ Cx45$^{fl/fl}$ mice (Suppl. Fig. 2).

4. Discussion

Results presented in this work indicate that Cx HCs mediate damage and dysfunction in skeletal muscles of blAJ mice, an animal model of human dysferlinopathy. In this animal model, we evaluated several parameters that were previously reported to be altered and are characteristic of dysferlinopathy. They included myofiber changes such as reduction in cross sectional area, presence of internal nuclei [37], elevated intracellular basal Ca^{2+} signals [8,17,28], lipid accumulation [14,15], as well as the elevation of serum CK [38]. In addition, we found an elevated sarcolemma permeability to small molecules. Surprisingly, all changes were completely absent in blAJ myofibers deficient in Cx43 and Cx45 expression, which were generated by crossing dysferlin deficient mice (blAJ) with mice bearing myofibers deficient in Cx expression (Cx43$^{fl/fl}$Cx45$^{fl/fl}$:M-C). These findings strongly suggest that important pathological mechanisms occur downstream the expression of these two Cxs, without ruling out the possible involvement of Cx39 HCs and other non-selective channels that might be co-expressed as it occurs after denervation [23] and sepsis [39], and lead to muscle degeneration and dysfunction in dysferlin deficiency.

The possible link between the absence or alteration of dysferlin and Cx HC expression remains to be elucidated. But we have recently shown that deficient activation of nicotinic acetyl choline receptor promotes expression of Cx HCs in skeletal myofibers [40]. Consequently, we speculate that a similar mechanism could operate in dysferlin deficient mice. In support to this possibility, it has been shown that presynaptic dysferlin deficiency drastically reduces the ACh release and promotes muscle changes reminiscent of LGMD2B disease [41] that corresponds to the dysferlinopathy of interest in the present study. This possibility is also supported by the fact that dysferlin plays a critical role in the trafficking of other proteins [5], which in blAJ mice could include synaptic vesicle creating a pseudo denervation condition. This might also explain why Cx expression deficiency of myofibers in blAJ Cx43$^{fl/fl}$Cx45$^{fl/fl}$:M-C mice totally prevents the manifestation of pathologic signs characteristic of dysferlinopathy, which are different from those observed in the mdx mice, animal model of Duchenne muscular dystrophy, where Cx expression deficiency in myofibers only partially prevents the appearance of pathologic outcome [28].

One hypothesis for dysferlinopathy proposed by Bansal et al. [8] is that the absence of dysferlin due to mutations in *DYSF* impedes sarcolema repair of myofibers after damage. This is because dysferlin is a protein critically involved in membrane repair mechanisms. Therefore, its absence would be the cause of skeletal muscle damage in dysferlinopathy. However, Lostal et al. [10] successfully rescued membrane repair function by means of two mechanisms: 1) by generating transgenic mice that overexpress myoferlin (a protein homologous to dysferlin), which were later mated with dysferlin-null mice, and the

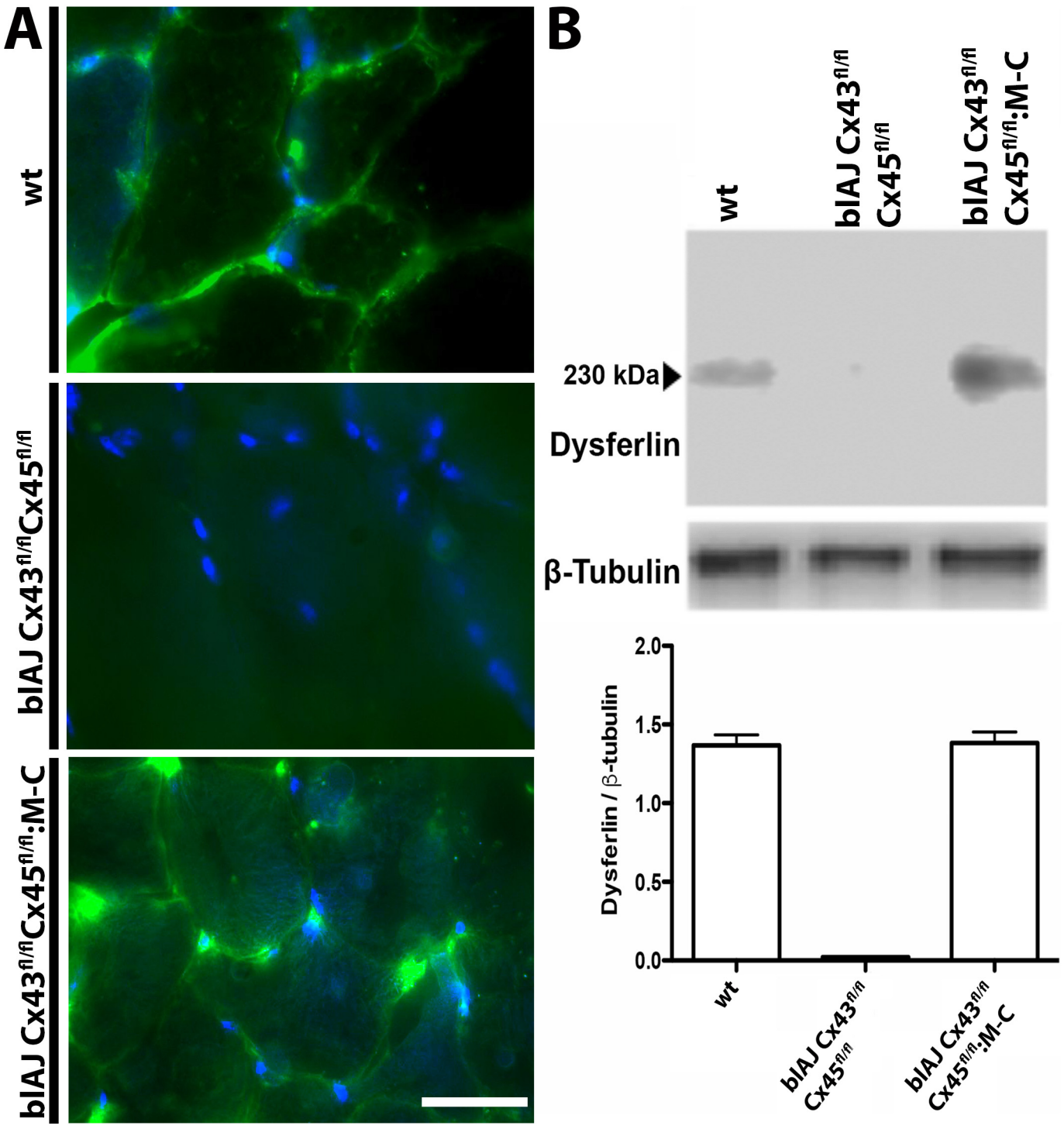

Fig. 8. Dysferlin reappears in blAJ muscles deficient in Cx43 and Cx45 expression. Dysferlin abundance from wild type (wt), blAJ and blAJ $Cx43^{fl/fl}Cx45^{fl/fl}$:M-C gastrocnemius muscles were analyzed by immunofluorescence and immunoblotting. A. Fast frozen cross sections of muscles were fixed and stained for dysferlin (Green). Positive signal (green signal) was detected in sections of muscles from wild type (wt) and blAJ $Cx43^{fl/fl}Cx45^{fl/fl}$:M-C mice but not from blAJ mice. Scale bar: 50 μm. B. A band at ~230 kDa (molecular mass of normal dysferlin) was detected in wt and in blAJ $Cx43^{fl/fl}Cx45^{fl/fl}$:M-C muscles. No band was detected in blAJ muscles. Bottom panel, quantification of relative amount of 230 kDa dysferlin band respect to β-Tubulin (dysferlin/ β-tubulin) from immunoblots as those shown in the upper panel. There are not significant differences in dysferin abundance between wt and blAJ $Cx43^{fl/fl}Cx45^{fl/fl}$:M-C muscles. n = 4 independent experiments.

generated mice presented normal membrane repair capacity, but muscular degeneration progressed invariably; and 2) by AAV-mediated transfer of a minidysferlin, previously shown to correct membrane repair deficit *in vitro*. These approaches, although successful in recovering membrane resealing capabilities, failed to improve muscle histology and arrest muscle wasting. The evidence strongly suggests the existence of another pathological mechanism triggered by the absence of dysferlin, in addition to that of membrane repair.

Another mechanism proposed for skeletal muscle damage in the absence of dysferlin is the activation of dihydropyridine receptors (DHPR). In this case, the damage is induced by osmotic shock in mouse dysferlin-deficient myofibers, which results in the functional and

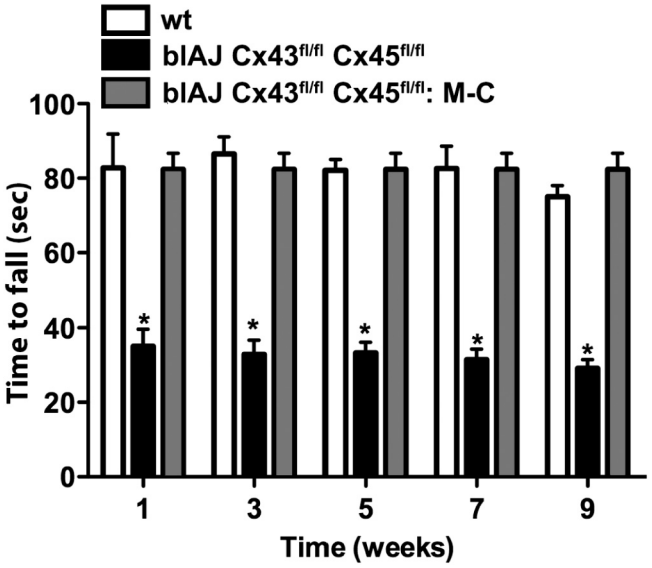

Fig. 9. Connexin hemichannels underlie poor motor performance of dysferlin deficient mice. Wild type (wt; white bar), blAJCx43$^{fl/fl}$Cx45$^{fl/fl}$ (black bar) and blAJ Cx43$^{fl/fl}$Cx45$^{fl/fl}$:M-C (grey bar) mice were challenged to a functional rotarod test. Time of resistance in the apparatus (time to fall, in seconds) was recorded for each animal. $n = 6$ animals per condition. *$P < 0.05$ respect to wt and blAJ Cx43$^{fl/fl}$ Cx45$^{fl/fl}$:M-C mice. Values represent means ± SEM.

structural disruption of the T-tubule structure, which in turn is ameliorated by the reduction of external [Ca^{2+}] or the blockade of L-type Ca^{2+} channels (DHPR) with diltiazem, hence prompting this inhibitor as a possible therapeutical drug [4]. However, chronic administration of diltiazem may be counterproductive, given that it is known to exert several side effects like alterations of skeletal muscular contraction, reduction of blood pressure and myocardial contractibility [42], as well as cutaneous adverse reactions [43]. Therefore, diltiazem has been discarded as a therapeutical option for dysferlinopathy. On the other hand, the removal of external Ca^{2+} stabilizes the T-tubule structure, suggesting that there is an influx of extracellular Ca^{2+} that is probably mediated by membrane channels. Again, DHPR could be a possible candidate due to the beneficial effects seen upon inhibition with diltiazem. However, the DHPR isoform present in skeletal muscle works as a voltage sensor, and not as a Ca^{2+} permeable channel [44]. The latter strongly suggests that other Ca^{2+} permeable membrane channels may account for increases in intracellular Ca^{2+} concentration, and their opening might be triggered by the activation of DHPR. In this sense, open Cx HCs have been shown to elevate basal intracellular Ca^{2+} concentrations in human dysferlin-deficient myotubes [28]. Here, we further demonstrated that Cx HCs contribute significantly to the increase in basal Ca^{2+} signal in skeletal myofibers from blAJ mice because myofibers of blAJ mice with myofibers deficient in Cx43 and Cx45 expression showed normal Ca^{2+} signal. It remains to be determined whether diltiazem blocks Cx HCs.

Elevated intracellular Ca^{2+} signal could in turn activate the inflammasome, ultimately promoting the inflammatory state and apoptosis of numerous myofiber known to occur in this disease [11]. These results suggest that normal Ca^{2+} buffering mechanisms are overwhelmed in dystrophic myofibers, and that the elimination of Cx HCs is sufficient to recover normal Ca^{2+} signaling. The presence of Cx HCs could also induce Na^+ influx, given that these channels are Na^+ permeable [29]. Elevating intracelular [Na^+] could in turn affect the function of Ca^{2+} extrusion systems like the Na^+/Ca^{2+} exchanger, as evidenced in other muscular dystrophies [45]. Consequently, avoiding increases in intracellular Ca^{2+} concentration *via* Cx HCs by removing Cx43 and Cx45 expression from skeletal myofibers prevented muscle atrophy and muscular degeneration, which in turn would reduce the amount of myofibers with internal nuclei. This led to a reduction in degeneration/regeneration cycles, and consequently the serum CK remained at normal values. High serum CK activity reflects sarcolemma disrupture most likely due to necrosis, which might result from intramuscle expansion of macrophages with cyto-destructive phenotype [46]. In addition, the inflammatory response might reduce repair and growth of myofibers causing uncoordinated muscle-bone growth, resulting in myofibers tear up by the continuous force imposed by bones undergoing growth.

It has been shown that myofibers of patients suffering dysferlinopathy present increased activity of protein degradation pathways [47]. Thus, the absence of dysferlin in myofibers of blAJ mice is probably due to the activation of protein degradation pathways, which can be activated by elevated intracellular Ca^{2+} signal [34]. Given that removing Cx43 and Cx45 prevented the formation of Cx43 and Cx45 HCs, which are permeable to Ca^{2+} [18,48], and consequently prevented the increase of intracellular Ca^{2+} signal and muscle atrophy, it is possible that Ca^{2+}-activated protein degradation pathways were not activated in myofibers of blAJ Cx43$^{fl/fl}$Cx45$^{fl/fl}$: M-C mice. It should be highlighted that blAJ mice have a mutation that is a retrotransposon insertion in intron 4, which results in aberrant splicing and in the absence of the dysferlin protein, probably due to the activation of protein degradation pathways. The recovery of dysferlin immunoreactivity indicate that the mutation does not affect the protein domain recognized by the antibody used to detect the protein in muscle sections.

Interestingly, removing Cxs 43 and 45 HCs also prevented lipid accumulation in skeletal muscles, suggesting that these channels participate in relevant pathological mechanisms involved in dysferlinopathy, and could be the initiators of the pathology after mutations in the *DYSF* gene. Whether lack of Cx43 and Cx45 expression prevents a phenomenon such as transdifferentiation of myofibers to adipose tissue remains to be demonstrated. Even though the absence of Cx43 and Cx45 expression in myofibers prevented all the alterations studied that characterize a dysfernilopathy, we cannot rule out the possible contribution of Cx39 HCs since it has been shown that open Cx39 HCs reduce the resting membrane potential of cells (Vargas et al., 2017).

Finally, the absence of elevated values of serum CK activity and the normal performance of physical work were accomplished by eliminating only Cx43 and Cx45 expression in skeletal myofibers of blAJ mice. This suggests that the involvement of these Cxs either in the initiation or progression of the pathological condition was triggered by the expression of mutated dysferlin. It also suggests that changes promoted by mutated dsyferlin in other tissues [5] are not so critical in determining the final outcome of dysferlinopathy. Moreover, the expression of Cx39 in muscles of blAJ Cx43$^{fl/fl}$Cx45$^{fl/fl}$: M-C mice reveals that this protein is not critical for the manifestation of different feature of the dysferlinopathy, which in part might be related to the impermeability of Cx39 HCs to Ca^{2+} [51].

Low open probability of Cx HCs in cell types that express Cxs under physiological conditions, and the expression of Cxs in myofibers only under pathological states constitute optimal conditions under which the disease could be treated with Cx HC blockers without relevant negative side effects. Since muscular tissue presents a strong regeneration capacity [49], it would be expected that once Cx HCs are blocked the progression of the disease would also stop, and muscle performance could be recovered after regeneration. A putative pharmacological approach could be the administration of boldine, which has been recently shown to block Cx HCs in inflamed myofibers, and drastically reduced the number of Cx HCs in the sarcolemma during longer treatments [50].

Supplementary data to this article can be found online at https://doi.org/10.1016/j.bbadis.2020.165800.

CRediT authorship contribution statement

Gabriela Fernández: Investigation, Data curation. **Guisselle Arias-Bravo**: Investigation, Data curation. **Jorge A. Bevilacqua**:

Writing - original draft. **Mario Castillo-Ruiz:** Investigation. **Pablo Caviedes:** Writing - original draft. **Juan C. Sáez:** Conceptualization, Writing - review & editing. **Luis A. Cea:** Conceptualization, Writing - review & editing, Supervision, Project administration.

Declaration of competing interest

The authors declare that they have no known competing financial interests or personal relationships that could have appeared to influence the work reported in this paper.

Acknowledgements

We thank Mr. Guillermo Elorza for his technical support. This work was partially supported by Fondo Nacional de Desarrollo Científico y Tecnológico (FONDECYT): Grant 11160739 (to LAC), Grants 1150291 and 1192329 (to JCS), Rings grant ACT 1121 (PIA, Conicyt, to PC and JAB) and Basal Centre, CeBiB, FB0001 and P09-022-F from ICM-ECONOMIA, Chile (to JCS). We also acknowledge to Jain Foundation USA by the generous donation of blAJ mice.

References

[1] G. Cenacchi, M. Fanin, L.B. De Giorgi, C.J. Angelini, Ultrastructural changes in dysferlinopathy support defective membrane repair mechanism, Clin Pathol. 58 (2) (2005) 190–195.
[2] L.V. Anderson, K. Davison, J.A. Moss, C. Young, M.J. Cullen, J. Walsh, M.A. Johnson, R. Bashir, S. Britton, S. Keers, Z. Argov, I. Mahjneh, F. Fougerousse, J.S. Beckmann, K.M. Bushby, Dysferlin is a plasma membrane protein and is expressed early in human development, Hum. Mol. Genet. 8 (5) (1999) 855–861.
[3] C. Matsuda, Y.K. Hayashi, M. Ogawa, M. Aoki, K. Murayama, I. Nishino, I. Nonaka, K. Arahata, R.H. Brown Jr., The sarcolemmal proteins dysferlin and caveolin-3 interact in skeletal muscle, Hum. Mol. Genet. 10 (17) (2001) 1761–1766.
[4] J.P. Kerr, A.P. Ziman, A.L. Mueller, J.M. Muriel, E. Kleinhans-Welte, J.D. Gumerson, S.S. Vogel, C.W. Ward, J.A. Roche, R.J. Bloch, Dysferlin stabilizes stress-induced Ca2+ signaling in the transverse tubule membrane, Proc. Natl. Acad. Sci. U. S. A. 110 (51) (2013) 20831–20836.
[5] C. Leung, S. Utokaparch, A. Sharma, C. Yu, T. Abraham, C. Borchers, P. Bernatchez, Proteomic identification of dysferlin-interacting protein complexes in human vascular endothelium, Biochem. Biophys. Res. Commun. 415 (2) (2011) 263–269.
[6] J.A. Urtizberea, G. Bassez, F. Leturcq, K. Nguyen, M. Krahn, N. Levy, Dysferlinopathies, Neurol. India 56 (3) (2008) 289–297.
[7] G. Galassi, L.P. Rowland, A.P. Hays, L.C. Hopkins, S. Di Mauro, High serum levels of creatine kinase: asymptomatic prelude to distal myopathy, Muscle Nerve 10 (4) (1987) 346–350.
[8] D. Bansal, K. Miyake, S.S. Vogel, S. Groh, C.C. Chen, R. Williamson, P.L. McNeil, K.P. Campbell, Defective membrane repair in dysferlin-deficient muscular dystrophy, Nature. 423 (6936) (2003) 168–172.
[9] L. Klinge, S. Laval, S. Keers, F. Haldane, V. Straub, R. Barresi, K. Bushby, From T-tubule to sarcolemma: damage-induced dysferlin translocation in early myogenesis, FASEB J. 21 (8) (2007) 1768–1776.
[10] W. Lostal, M. Bartoli, C. Roudaut, N. Bourg, M. Krahn, M. Pryadkina, P. Borel, L. Suel, J.A. Roche, D. Stockholm, R.J. Bloch, N. Levy, R. Bashir, I. Richard, Lack of correlation between outcomes of membrane repair assay and correction of dystrophic changes in experimental therapeutic strategy in dysferlinopathy, PLoS One 7 (5) (2012) e38036.
[11] R. Rawat, T.V. Cohen, B. Ampong, D. Francia, A. Henriques-Pons, E.P. Hoffman, K. Nagaraju, Inflammasome up-regulation and activation in dysferlin-deficient skeletal muscle, Am. J. Pathol. 176 (6) (2010) 2891–2900.
[12] J.P. Kerr, C.W. Ward, R.J. Bloch, Dysferlin at transverse tubules regulates Ca(2+) homeostasis in skeletal muscle, Front. Physiol. 5 (2014) 89.
[13] J.R. Terrill, H.G. Radley-Crabb, T. Iwasaki, F.A. Lemckert, P.G. Arthur, M.D. Grounds, Oxidative stress and pathology in muscular dystrophies: focus on protein thiol oxidation and dysferlinopathies, FEBS J. 280 (17) (2013) 4149–4164.
[14] M.D. Grounds, J.R. Terrill, H.G. Radley-Crabb, T. Robertson, J. Papadimitriou, S. Spuler, T. Shavlakadze, Lipid accumulation in dysferlin-deficient muscles, Am. J. Pathol. 184 (6) (2014) 1668–1676.
[15] K. Kobayashi, T. Izawa, M. Kuwamura, J. Yamate, The distribution and characterization of skeletal muscle lesions in dysferlin-deficient SJL and A/J mice, Exp. Toxicol. Pathol. 62 (5) (2010) 509–517.
[16] R.A. Bannister, I.N. Pessah, K.G. Beam, The skeletal L-type Ca^{2+} current is a major contributor to excitation-coupled Ca^{2+} entry, J Gen Physiol. 133 (1) (2009) 79–91.
[17] L.A. Cea, J.A. Bevilacqua, C. Arriagada, A.M. Cárdenas, A. Bigot, V. Mouly, J.C. Sáez, P. Caviedes, The absence of dysferlin induces the expression of functional connexin-based hemichannels in human myotubes, BMC Cell Biol. 17 (Suppl. 1) (2016) 15.
[18] K.A. Schalper, H.A. Sánchez, S.C. Lee, G.A. Altenberg, M.H. Nathanson, J.C. Sáez, Connexin 43 hemichannels mediate the Ca^{2+} influx induced by extracellular alkalinization, Am J Physiol Cell Physiol. 299 (6) (2010) C1504–C1515.
[19] S. Ramachandran, L.H. Xie, S.A. John, S. Subramaniam, R. Lal, A novel role for connexin hemichannel in oxidative stress and smoking-induced cell injury, PLoS One 2 (8) (2007) e712.
[20] N. Belluardo, A. Trovato-Salinaro, G. Mudò, D.F. Condorelli, Expression of the rat connexin 39 (rCx39) gene in myoblasts and myotubes in developing and regenerating skeletal muscles: an in situ hybridization study, Cell Tissue Res. 320 (2) (2005) 299–310.
[21] J. von Maltzahn, C. Euwens, K. Willecke, G. Söhl, The novel mouse connexin39 gene is expressed in developing striated muscle fibers, J. Cell Sci. 117 (Pt 22) (2004) 5381–5392.
[22] L.A. Cea, M.A. Riquelme, B.A. Cisterna, C. Puebla, J.L. Vega, M. Rovegno, J.C. Sáez, Connexin- and pannexin-based channels in normal skeletal muscles and their possible role in muscle atrophy, J. Membr. Biol. 245 (8) (2012) 423–436.
[23] L.A. Cea, B.A. Cisterna, C. Puebla, M. Frank, X.F. Figueroa, C. Cardozo, K. Willecke, R. Latorre, J.C. Sáez, De novo expression of connexin hemichannels in denervated fast skeletal muscles leads to atrophy, Proc. Natl. Acad. Sci. U. S. A. 110 (40) (2013) 16229–16234.
[24] M.A. Riquelme, L.A. Cea, J.L. Vega, M.P. Boric, H. Monyer, M.V. Bennett, M. Frank, K. Willecke, J.C. Sáez, The ATP required for potentiation of skeletal muscle contraction is released via pannexin hemichannels, Neuropharmacology. 75 (2013) 594–603.
[25] C. Anderson, H. Catoe, R. Werner, MIR-206 regulates connexin43 expression during skeletal muscle development, Nucleic Acids Res. 34 (20) (2006) 5863–5871.
[26] L.A. Cea, M.A. Riquelme, A.A. Vargas, C. Urrutia, J.C. Sáez, Pannexin 1 channels in skeletal muscles, Front. Physiol. 5 (2014) 139.
[27] Cardiff, Robert H. Miller, Claramae, J. Munn, Robert, Manual hematoxylin and eosin staining of mouse tissue sections, Cold Spring Harb Protoc 2014 (2014).
[28] L.A. Cea, C. Puebla, B.A. Cisterna, R. Escamilla, A.A. Vargas, M. Frank, P. Martínez-Montero, C. Prior, J. Molano, I. Esteban-Rodríguez, I. Pascual, P. Gallano, G. Lorenzo, H. Pian, L.C. Barrio, K. Willecke, J.C. Sáez, Fast skeletal myofibers of mdx mouse, model of Duchenne muscular dystrophy, express connexin hemichannels that lead to apoptosis, Cell. Mol. Life Sci. 73 (13) (2016) 2583–2599.
[29] S. Li, M.P. Czubryt, J. McAnally, R. Bassel-Duby, J.A. Richardson, F.F. Wiebel, A. Nordheim, E.N. Olson, Requirement for serum response factor for skeletal muscle growth and maturation revealed by tissue-specific gene deletion in mice, Proc. Natl. Acad. Sci. U. S. A. 102 (4) (2005) 1082–1087.
[30] R. Koopman, G. Schaart, M.K. Hesselink, Optimisation of oil red O staining permits combination with immunofluorescence and automated quantification of lipids, Histochem. Cell Biol. 116 (1) (2001) 63–68.
[31] T. Inai, Y. Shibata, Heterogeneous expression of endothelial connexin (Cx) 37, Cx40, and Cx43 in rat large veins, Anat. Sci. Int. 84 (3) (2009) 237–245.
[32] V.J. Schmidt, A. Jobs, J. von Maltzahn, P. Wörsdörfer, K. Willecke, C. de Wit, Connexin45 is expressed in vascular smooth muscle but its function remains elusive, PLoS One 7 (7) (2012) e42287.
[33] S. Gehlert, W. Bloch, F. Suhr, Ca^{2+}-dependent regulations and signaling in skeletal muscle: from electro-mechanical coupling to adaptation, Int. J. Mol. Sci. 16 (1) (2015) 1066–1095.
[34] R. Mukherjee, A. Das, S. Chakrabarti, O. Chakrabarti, Calcium dependent regulation of protein ubiquitination - interplay between E3 ligases and calcium binding proteins, Biochim Biophys Acta Mol Cell Res. 1864 (7) (2017) 1227–1235.
[35] E.S. Folker, M.K. Baylies, Nuclear positioning in muscle development and disease, Front. Physiol. 4 (2013) 363.
[36] M.A. Hornsey, S.H. Laval, R. Barresi, H. Lochmüller, K. Bushby, Muscular dystrophy in dysferlin-deficient mouse models, Neuromuscul. Disord. 23 (5) (2013) 377–387.
[37] N.J. Patel, K.W. Van Dyke, L.R. Espinoza, Limb-girdle muscular dystrophy 2B and Miyoshi presentations of dysferlinopathy, Am J Med Sci. 353 (5) (2017) 484–491.
[38] H. Jethwa, T.S. Jacques, R. Gunny, L.R. Wedderburn, C. Pilkington, A.Y. Manzur, Limb girdle muscular dystrophy type 2B masquerading as inflammatory myopathy: case report, Pediatr Rheumatol Online J. 11 (1) (2013) 11–19.
[39] E. Balboa, F. Saavedra, L.A. Cea, A.A. Vargas, V. Ramírez, R. Escamilla, J.C. Sáez, T. Regueira, Sepsis-induced channelopathy in skeletal muscles is associated with expression of non-selective channels, Shock. 49 (2) (2018) 221–228.
[40] B.A. Cisterna, A. Vargas, C. Puebla, P. Fernández, R. Escamilla, C. Lagos, M. Matus, C. Vilos, L.A. Cea, E. Barnafi, H. Gaete, D. Escobar, C. Cardozo, J.C. Sáez, Active acetylcholine receptors prevent the atrophy of skeletal muscles and favor reinnervation, Nat. Commun. 11 (1) (2020) 1073.
[41] P. Krajacic, E.E. Pistilli, J.E. Tanis, T.S. Khurana, S.T. Lamitina, FER-1/Dysferlin promotes cholinergic signaling at the neuromuscular junction in C. elegans and mice, Biol Open. 2 (11) (2013) 1245–1252.
[42] W.E. Boden, M. Vray, E. Eschwege, D. Lauret, R. Scheldewaert, Heart rate-lowering and -regulating effects of once-daily sustained-release diltiazem, Clin. Cardiol. 24 (1) (2001) 73–79.
[43] P. Tuchinda, K. Kulthanan, S. Khankham, K. Jongjarearnprasert, N. Dhana, Cutaneous adverse reactions to calcium channel blockers, Asian Pac. J. Allergy Immunol. 32 (3) (2014) 246–250.
[44] R.A. Bannister, K.G. Beam, Ca(V)1.1: the atypical prototypical voltage-gated Ca^{2+} channel, Biochim. Biophys. Acta 1828 (7) (2013) 1587–1597.
[45] M. Yoshida, A. Yonetani, T. Shirasaki, K. Wada, Dietary NaCl supplementation prevents muscle necrosis in a mouse model of Duchenne muscular dystrophy, Am J Physiol Regul Integr Comp Physiol. 290 (2) (2006) R449–R455.
[46] J.H. Baek, G.M. Many, F.J. Evesson, V.R. Kelley, Dysferlinopathy promotes an intramuscle expansion of macrophages with a cyto-destructive phenotype, Am. J. Pathol. 187 (6) (2017) 1245–1257.
[47] M. Fanin, A.C. Nascimbeni, C. Angelini, Muscle atrophy, ubiquitin-proteasome, and autophagic pathways in dysferlinopathy, Muscle Nerve 50 (3) (2014) 340–347.

[48] K.A. Schalper, N. Palacios-Prado, M.A. Retamal, K.F. Shoji, A.D. Martínez, J.C. Sáez, Connexin hemichannel composition determines the FGF-1-induced membrane permeability and free [Ca^{2+}]i responses, Mol. Biol. Cell 19 (8) (2008) 3501–3513.
[49] A. Wernig, R. Schäfer, U. Knauf, R.R. Mundegar, M. Zweyer, O. Högemeier, U.M. Martens, S. Zimmermann, On the regenerative capacity of human skeletal muscle, Artif. Organs 29 (3) (2005) 192–198.
[50] L.A. Cea, E. Balboa, A.A. Vargas, C. Puebla, M.C. Brañes, R. Escamilla, T. Regueira, J.C. Sáez, De novo expression of functional connexins 43 and 45 hemichannels increases sarcolemmal permeability of skeletal myofibers during endotoxemia, Biochim. Biophys. Acta Mol. basis Dis. 1865 (10) (2019) 2765–2773.
[51] A.A. Vargas, B.A. Cisterna, F. Saavedra-Leiva, C. Urrutia, L.A. Cea, A.H. Vielma, S.E. Gutierrez-Maldonado, A.J. Martin, C. Pareja-Barrueto, Y. Escalona, O. Schmachtenberg, C.F. Lagos, T. Perez-Acle, JC. Sáez, On Biophysical Properties and Sensitivity to Gap Junction Blockers of Connexin 39 Hemichannels Expressed in HeLa Cells, Front Physiol 8 (38) (2017).